# Experimental and numerical study on the mechanical behaviour of CLT shearwalls with openings

Daniele Casagrande[1*], Riccardo Fanti[1], Ghasan Doudak[2], Andrea Polastri[1]

[1]Institute of Bioeconomy - National Research Council of Italy; daniele.casagrande@ibe.cnr.it; andrea.polastri@ibe.cnr.it; riccardo.fanti@ibe.cnr.it; *Corresponding Author

[2]University of Ottawa, Canada; gdoudak@uottawa.ca;

## Abstract

An investigation of the mechanical behaviour of CLT shearwalls, where either door or window openings are cut out of the panel, is undertaken. The main aim of the study is to investigate failure modes related to either mechanical anchor or CLT panel, based on the geometrical dimensions and mechanical properties of shearwall. The results of six full-scale monolithic CLT shearwalls with window or door openings are presented and discussed. The results obtained from the full-scale shearwall tests are used to validate a proposed numerical model, where input parameters, such as the mechanical properties of the CLT panels and mechanical anchors, are obtained from component level tests on beams and connections in isolation. The study shows that differently from single-panel shearwalls with no openings, brittle failure in the CLT panels is a possible mode of failure, which needs to be considered in design. The failure mode in the CLT panels is observed to occur either in bending or net shear in the lintel beams. The proposed numerical procedure is found capable of estimating the maximum load with reasonable accuracy, and the model predictions of the failure mode, number of centre of rotations, and the overall deformation of the CLT panel are accurate for all the studied specimens.

## Keywords

Shearwalls; openings; timber structures; numerical models; beam tests; Cross Laminated Timber.

## Highlights

- An investigation of the behaviour of CLT shearwalls with openings is undertaken.
- Failure modes related to either mechanical anchor or CLT panel are studied.
- Full-scale shearwall tests were used to validate a proposed numerical model.
- Input parameters for numerical model were obtained from component level tests.

# 1. Introduction

The high strength-to-weight ratio and in-plane stiffness of Cross Laminated Timber (CLT) panels, together with the ability of these structural systems to dissipate energy through mechanical connections, have made them a valuable alternative to other traditional materials, especially in seismic prone areas [1-2]. The appeal of using CLT shearwalls lies in the relative simplicity of the procedure used in the design method, where panels are assumed to possess superior (or infinite) in-plane stiffness, thereby engaging the boundary connections through rigid-body rotation and/or translation. Those boundary connections typically consist of relatively flexible and ductile fasteners connecting adjacent panels together, and mechanical anchors (angle brackets and hold-downs) that ensure the transfer of shear and overturning forces to lower storeys or foundation.

The connections between panel elements may be omitted in design cases where energy dissipation is not required (e.g. areas where wind loading governs design), and alternatively, the entire shearwall could consist of a single CLT panel. This provides an assembly that has very high stiffness and that is relatively easy to manufacture and assemble on site. The need to have window and door openings in the walls necessitate cutting such openings directly in the panels, and thereby facilitating the assembly process. Alternatively, the door and window spaces are accounted for during the erection process and header beams and parapets are installed separately following the installation of the wall segments. The difference in the behaviour, and consequently the analysis procedure and design assumptions, between these two systems is considerable. When the lintel beams and parapets are installed separately, it can generally be assumed that the wall segments behave as cantilevers, the CLT panels remain elastic, and the failure occurs in the mechanical anchors. Conversely, when the openings are cut out of the CLT wall panel, the structural continuity between lintels and wall segments is ensured and brittle failure in the CLT panels is a possible mode of failure that designers need to consider. The prediction of this type of failure is complicated by the presence of several factors, including variability in the wood material, the multiplicity of possible failure modes and the high stress concentration typically found at the edge of structural elements bordering the openings. The variability found in wood material could lead to a diminished ability to predict the failure mode with reasonable accuracy. Also, the difference between design level strength and in-situ strength of wood element is not well established in order to predict the sequence of failure between wood element and the mechanical anchors as well as different failure modes possibly to occur within the wood element. Furthermore, the theoretical stress level found near corners and edges of element may not always be actually present in the physical element or may not initiate the failure due to the reinforcing effects of the transverse laminates in CLT panels.

As will be demonstrated in the following section, several of the aforementioned issues related to single wall panels with openings have not been addressed in the literature. The main motivation of the current study is to investigate the mechanical behaviour of CLT shearwalls where either door or window openings are cut out of the panel. In particular, the study aims to investigate failure modes related to either mechanical anchor or CLT panel, based on the geometrical dimensions and mechanical properties of shearwall. The link between the mechanical behaviour of CLT beams with vertical outer layers and the behaviour of the CLT shearwall is also established through experimental testing and numerical analysis using finite element (FE) model.

The methodology used in the current study involves experimental investigation of six full-scale monolithic CLT shearwalls with window or door openings. The geometrical dimensions of shearwalls, layout of the CLT panels, size of openings and type of mechanical anchors were selected with the intention of achieving a targeted failure mode related to either the lintel beam or the mechanical anchors. The results obtained from the full-scale shearwall tests were used to validate a numerical model, where input parameters such as the mechanical properties of the CLT panels and mechanical anchors were obtained from component level tests on beams and connections in isolation. The effects of vertical load and potential uplift stiffen

ss and strength of angle brackets have been omitted from this investigation in order to reduce the variables on the study's focus, which relates to the failure mechanism, especially in the lintel beam. The comprehensiveness of the proposed model and accompanying experimental campaign will be achieved by incrementally introducing such parameters in ongoing and future research effort.

## 2. State of the art

Establishing the behaviour of CLT shearwalls without openings has been the subject of several research programmes in the past two decades. These studies have involved significant experimental components of shearwall assemblies in isolation as well as part of a system at the building level. Analytical and numerical approaches have also been developed to investigate the influence of mechanical connections on the structural performances of CLT buildings consisting of single- or multi-panel shearwalls. The main outcome from the experimental testing was the confirmation that the lateral behaviour of CLT shearwall without openings, at the ultimate limit state, is governed by the mechanical performance of connections, while the CLT panels can be assumed to behave almost elastically.

At the building level, Ceccotti et al. [3] performed shake-table tests on a 7-storey CLT building constructed with primarily multi-panel shearwalls. Tsuchimoto et al. [4] experimentally investigated the static and dynamic response of a 3-storey CLT structure with semi-rigid connections between wall segments and lintel beams demonstrating adequate seismic performance. Flastcher and Schickhofer [5] investigated the seismic performance of a 3-storey CLT building with single-panel shearwalls using a shake-table. The main finding from this study was that multi-panel CLT shearwalls experienced more deformation but also more ductility than those consisting of a single panel. Popovski and Gavric [6] studied the lateral behaviour of a 2-storey CLT building under monotonic and cyclic loading. The building was characterized by single-panel CLT shearwalls with openings cut out of the panels in one direction, while multi-panels shearwalls were adopted along the other direction. The failure was characterized by nail yielding in the brackets at the base of the wall due to combined action of rocking and sliding. Significant slip along the vertical joints in multi-panel shearwalls was detected. Van de Lindt et al. [7] performed shake-table tests on a 2-storey CLT timber building in order to investigate the influence of panel aspect ratios and presence of perpendicular CLT walls. The results showed that shearwalls with high values of panel aspect ratio were governed by rocking failure, while shearwalls with low values of panel aspect ratio were characterized mainly by sliding mechanism. It was also observed that the perpendicular walls did not significantly affect the rocking behaviour of shearwalls. Gavric and Popovski [32] evaluated the influence of the perpendicular walls on the strength capacity of CLT shearwalls through experimental cyclic tests on a 2-storey CLT house. The results showed that the perpendicular walls increased the rocking strength capacity of shearwall and altered the failure condition in most of the shearwalls to that of sliding.

A significant number of experimental studies have also been undertaken at the wall level primarily for CLT shearwalls without openings. Popovski et al. [8] conducted quasi-static tests on single- and multi-panel shearwalls, characterised by different wall aspect ratios. The study also investigated two-storey wall assemblies. The results from this investigation showed that the energy dissipation and ductility capacity of single-panel shearwalls is related to the mechanical behaviour of hold-down and angle-brackets. Hristovski et al. [9] performed shake-table tests on both single- and multi-panel CLT shearwalls showing that the mechanical anchors are able to dissipate adequate seismic energy when a rocking behaviour is exhibited by shearwalls. Okabe et al. [10] studied the influence of vertical load on the rocking behaviour of single- and multiple-panel walls, concluding that vertical load can significantly increase the strength capacity of CLT shearwalls. Gavric et al. [11] investigated the cyclic behaviour of both single- and multi-panel shearwalls, reporting that the in-plane deformations of the CLT panels were almost negligible and that the failure mode and inelastic deformations were limited to the mechanical anchors and vertical joints. Akbas et al. [12] studied the behaviour of self-centering CLT shearwalls connected to the foundation by means of vertical post-tensioned steel bars. The study also provided simple analytical expressions for the prediction of the lateral response of such structural systems. Cyclic and monotonic tests were also conducted by Chen and Popvoski [13] on balloon-type CLT sherwalls in order to validate a proposed mechanics-based analytical model to predict the lateral response of such walls. The experimental tests showed that coupled-panel balloon-type CLT shearwalls with semi-rigid and ductile vertical joints possess much larger plastic deformations than those consisting of single-panel shearwalls. D'Arenzo et al. [14] investigated the lateral behaviour of CLT shearwalls connected to the floor below by means of innovative bi-directional angle brackets. The study showed a comparable mechanical behaviour of the tested shearwalls with those using traditional hold-down and angle brackets.

Research conducted on shearwalls with openings has been relatively limited and, in most cases, aimed only at defining reduction coefficients that take into account the effect of opening dimensions on the stiffness and strength capacity of shearwall. Dujic et al [15] presented the results of experimental and parametric numerical analyses of CLT shearwalls with different size and configuration of door and window openings.

Studies by Ceccotti et al. [16] and Flatscher et al. [17] presented results from shearwalls with a door opening, where failure was observed in the mechanical anchors used to connect shearwalls to the foundation, while the CLT panels behaved elastically. Yasamura et al. [18] investigated a 2-storey CLT buildings constructed using single-panel shearwalls with openings and reported observations of failure in the mechanical anchors used to prevent the uplift of panels as well as the formation of cracks at corners of the openings. The study emphasized the importance of considering the panel failure in the design of CLT panels with openings. Pai et al. [19] numerically investigated the force transfer around openings in CLT shearwalls and identified the needs for local reinforcements to avoid premature failure in the panel. Mestar et al. [20] established the kinematic modes of shearwalls with door or window openings, based on the hold-down configuration and the geometrical dimensions of the CLT panels. The experimental tests showed that failure mostly occurred in the hold-down while bending failure in the CLT panel was observed in wall with door opening and high length-to-height aspect ratio of the lintel beam.

Most of the numerical studies on CLT shearwalls with openings aimed at determining reduction coefficients to be applied to an equivalent CLT shearwall with no openings [21-23]. Generally, 2-D area elements were implemented in the finite element models to represent the behaviour of the CLT panels. An equivalent frame model was proposed by Mestar et al. [24], as an alternative to the FE model with 2D area elements, to establish the behaviour of CLT shearwalls with window or door openings.

Review of the available literature makes it clear that although a significant effort has been made to establish the behaviour of CLT shearwalls with various geometrical configurations and connection detailing, there is a clear gap in knowledge in relation to the behaviour of monolithic shearwalls with openings. Studies on these structural systems have been scarce and limited in scope to observations of various failure modes, with little emphasis on failure occurring in the CLT panel. Such failure modes are naturally brittle and should be avoided, and hence need to be better understood. To the authors' knowledge, no experimental study has been undertaken with the aim to specifically achieve a targeted failure in the CLT panel. The current study aims to establish a better understanding of the behaviour of key parameters affecting the shearwall performance, such as lintel beams and mechanical anchors, in isolation as well as part of the wall assembly.

# 3. Experimental test set-up

In this section, the tests conducted on full-scale CLT shearwalls with openings and those undertaken at the component level on CLT beams and mechanical anchors are described.

## 3.1 Tests on shearwalls

Monotonic tests were carried out on six CLT shearwalls with either door or window openings. The openings were cut out from CLT panels in order to maintain structural continuity between the wall segments and the lintel beam and parapet. The panels comprised of Spruce boards of C24 grade and width, *w,* of 170 mm, manufactured according to [33]. The total thickness, $t_{tot}$, of 3- and 5-ply panels were 90 mm and 100 mm, with layout of laminations of 30v-30h-30v and 20v-20h-20v-20h-20v, respectively. The designation "*v*" and "*h*" here indicate the orientation of the lamination being vertical and horizontal, respectively.

The wall height, $h_{\mathrm{wall}}$, was equal to 2380 mm for all shearwall test specimens. Commercially available hold-down anchors (WHT620) were used to connect the wall to a steel base beam, representing the foundation. Each hold-down was connected to the wall panel using fifty-five 4x60 mm ring shanked nails, while the attachment to the steel base beam was achieved using an M20 bolt. Two different hold-down configurations were adopted: a double hold-down configuration (DH), where hold-down anchors were placed at both ends of each wall segments, and single hold-down configuration (SH), where hold-downs were placed at the ends of the shearwall. The choice of investigating these hold-down configurations was based on the results obtained by Mestar et al. [20], which presented different kinematic behaviour of the wall based on the hold-down configuration.

The geometrical dimensions and the opening layouts of the wall specimens are presented in Table 1 and shown in Figure 1. As seen in Table 1, a label is presented for each specimen, indicating the type of opening being a door or window (D or W), number of lamination layers in the CLT panel (3 or 5), and whether the lintel is considered to be relatively short or long with respective lengths of 600 mm or 900 mm (S) and 1500 mm (L). Using this terminology, a specimen with label W_5_S would consist of a window opening where the panels comprise of 5-ply CLT and a short lintel beam. In Table 1, the variable $l_{wall}$ represents the total length of the shearwall, $l_{op}$ is the length of the opening, while $h_{lintel}$ and $h_{par}$ are the height of the lintel and parapet, respectively. Figure 2 also shows a photograph of the test setup using wall specimens 02 and 06 as examples. It can be noted in Figure 2 that the hold-down connection farthest away from the load application point is always assumed to be subjected to a compression force and has therefore been omitted.

**Table 1:** *layout of shearwall tests*

| Test | Label | n. of layers [-] | $t_{tot}$ [mm] | $l_{wall}$ [mm] | $h_{lintel}$ [mm] | $h_{par}$ [mm] | $l_{op}$ [mm] | Opening type [-] | Hold-down config. [-] |
|---|---|---|---|---|---|---|---|---|---|
| Wall 01 | D_3_S | 3 | 90 | 3300 | 340 | - | 600 | Door | SH |
| Wall 02 | D_5_S | 5 | 100 | 3300 | 340 | - | 900 | Door | DH |
| Wall 03 | W_5_S | 5 | 100 | 3300 | 340 | 340 | 900 | Window | SH |
| Wall 04 | D_3_L | 3 | 90 | 3900 | 510 | - | 1500 | Door | DH |
| Wall 05 | D_5_L | 5 | 100 | 3900 | 340 | - | 1500 | Door | DH |
| Wall 06 | W_5_L | 5 | 100 | 3900 | 340 | 340 | 1500 | Window | DH |

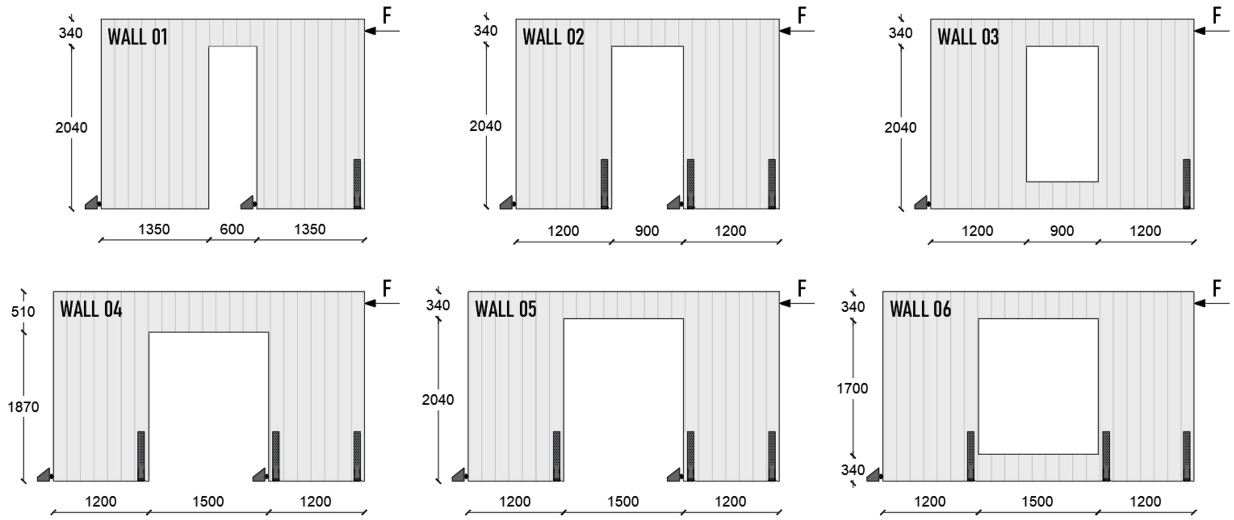


**Figure 1:** *Geometrical dimensions and the opening layout*

a) b)

**Figure 2:** *wall 02 D_5_S (a) and wall 06 W_5_L (b)*

Figure 3a provides important details on the blocking mechanism that was adopted in the test set-up in order to prevent the sliding of shearwall. The blocking consisted of a 15 mm thick steel plate, designed to prevent the development of localized high compression stresses in the wood, while a cylindrical steel section acted as a roller to allow free rotation of the wall. The lateral load was applied by means of a horizontal hydraulic jack, connected to a rigid steel frame. A 25 mm thick steel plate was used to transfer the load from the hydraulic jack to the top corner of the wall, as shown in Figure 3b.

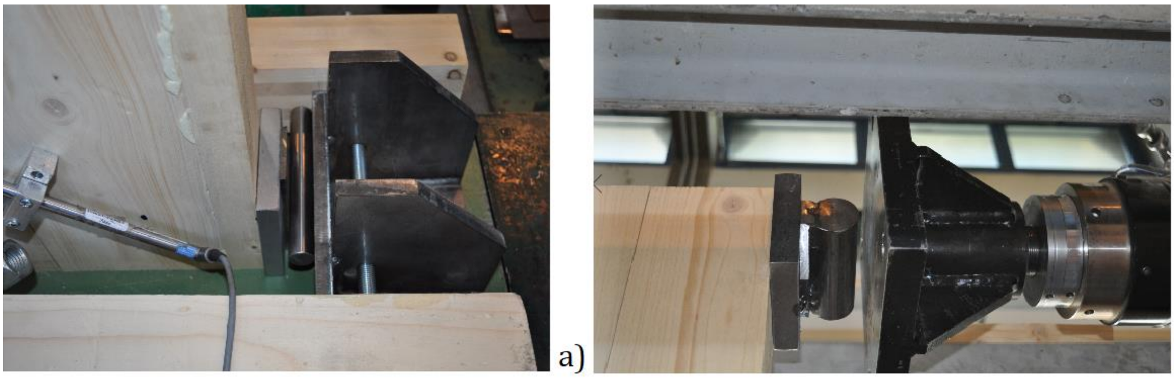

a) b)

**Figure 3:** *blocking mechanism at the bottom of the wall (a) and steel plate at the top of the wall (b)*

Additional restraints were provided at the top of the wall specimen, on both sides, to prevent out-of-plane movement of the wall and buckling of the lintel beam (see Figure 2). The testing procedure was carried out in accordance with the EN594 standard [25]. It is noteworthy to mention that the vertical load has been omitted in the current testing program, in order to study the behaviour of the wall with opening using fewer parameters. It can be expected that the vertical load would provide a stabilizing effect on the rocking behaviour of the wall, while increasing the shear and bending forces in lintel elements, which in turn could lead to an increased probability of failure occurring in CLT panels. It is recommended that future studies be carried out to investigate the role and impact of the vertical load on the behaviour of the wall system. Figure 4 shows the instrumentation layout to capture the various deformation contributions of the CLT panel and the mechanical anchors. Two Linear Variable Displacements Transducers (LVDTs) were used to measure the horizontal displacements $\delta_{TOP,1}$ and $\delta_{TOP,2}$ at the top of shearwall at each end (LVDT 1 and 2), while another LVDT (either 3 or 4) was positioned horizontally at the bottom of the wall to measure its sliding displacement $\delta_{BOT}$. Two additional LVDTs (5 and 6) were used to measure the uplift displacement $V_1$ and $V_2$ at the bottom corner of the first wall segment (i.e. that closest to the load application point and most prone to uplift). LVDTs 7 and 8 were connected to two diagonal wires in order to measure the panel deformation $d_T$ and $d_C$. The relative top horizontal displacement of the wall, $\delta$, was obtained by calculating the difference between the top horizontal displacement measured by LVTD 1 or 2 (i.e. $\delta_{TOP,1}$ or $\delta_{TOP,2}$) and the sliding measured at the bottom of the wall, $\delta_{BOT}$.

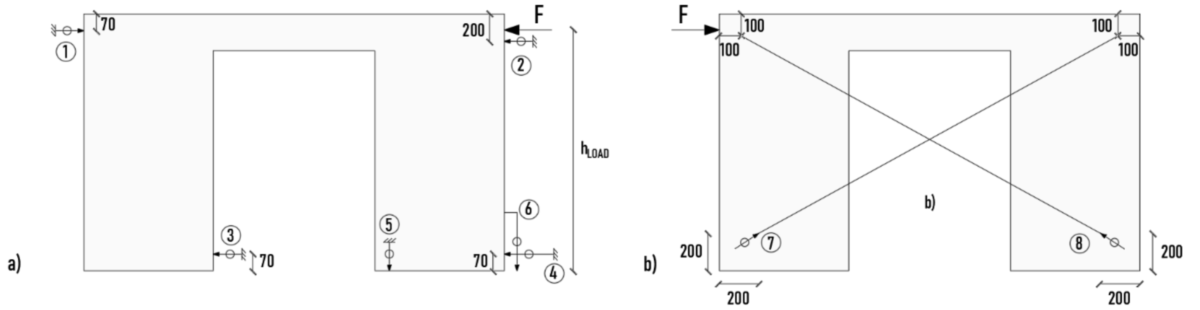


**Figure 4:** *test measurement (front, a, and back, b)*

3.2 Component-level tests

As mentioned before, the purpose of conducting component level tests was to obtain a more accurate input parameters for the numerical model and to minimize the variability usually associated with failure in the wood material.

The CLT beam were selected from same batch as the CLT wall panels and they had the same layup pattern, number of layers (3 and 5), orientation of laminates (Figure 5), species (spruce) as well as grade (C24), manufactured according to [33]. The thickness of the beams and width of individual boards were selected such that they were consistent with the full-scale shearwall specimens. The beam height, *h,* was chosen to be a multiple of the board width, *w*, (i.e. *h*=2x170=340 mm). The specimen configurations consisted of two different lengths, namely equal to 4.76 m and 2.72 m, in order to promote bending and shear failure modes, respectively.

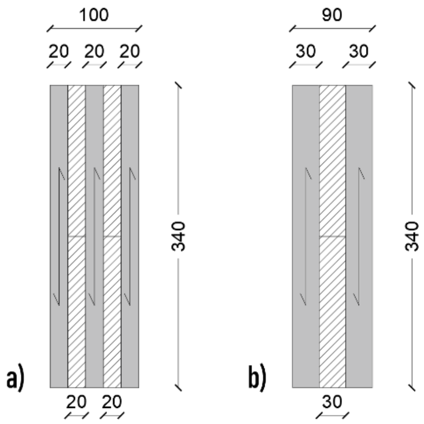


**Figure 5:** *cross section of beam specimen with 5- (a) and 3-layers (b)*

The geometrical dimensions of the CLT beams and the number of specimens for each configuration are reported in Table 2, where the thickness and orientation of the individual laminations are also provided. Variables $t_h$ and $t_v$ represent the total thickness of laminations along the horizontal and vertical direction, respectively.

**Table 2:** *layup of specimens*

| $l_{beam}$ = 4760 mm | | | | | | |
|---|---|---|---|---|---|---|
| Specimen number | n. of specimen | n. of layers | Layup [mm] | $t_h$ [mm] | $t_v$ [mm] | $t_{TOT}$ [mm] |
| B 01 | 3 | 5 | 20v-20h-20v-20h-20v | 40 | 60 | 100 |
| B 02 | 3 | 3 | 30v-30h-30v | 30 | 60 | 90 |
| $l_{beam}$ = 2720 mm | | | | | | |
| Specimen number | n. of specimen | n. of layers | Layup [mm] | $t_h$ [mm] | $t_v$ [mm] | $t_{tot}$ [mm] |
| B 03 | 3 | 5 | 20v-20h-20v-20h-20v | 40 | 60 | 100 |
| B 04 | 3 | 3 | 30v-30h-30v | 30 | 60 | 90 |

Figure 6 shows the test setup and boundary conditions for the beam tests. Each beam was supported on steel rollers and loaded at the third points between the two bearing supports. The load was applied up to the specimen failure using a 250 kN hydraulic jack at a constant rate in accordance with EN408 [26]. Two LVDTs, one on each side of the beam, were used to measure the total vertical deflection, $w_{glob}$, at the mid-span, while two other LVDTs measured the local relative displacement, $w_{loc}$, between the centre of the beam and a fixed point located in the null-shear zone in conformance with EN408 [26].

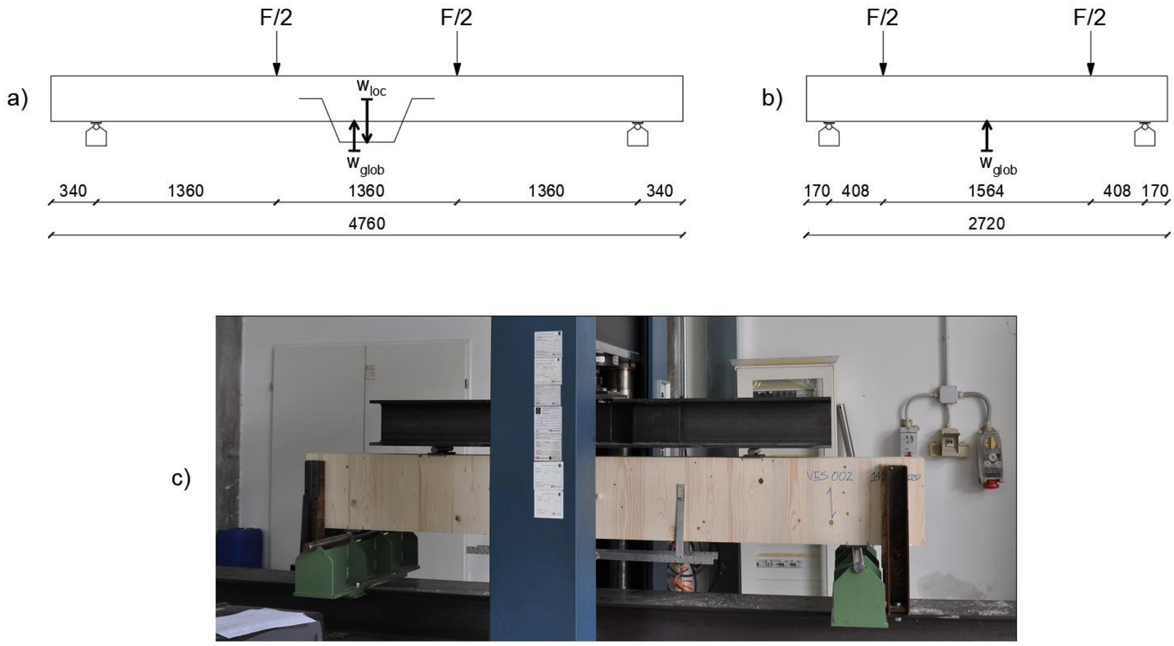


**Figure 6:** *the test set-ups (a and b) and bending test B 04 (specimen 002) (c)*

Two monotonic tests were carried out on the same hold-down anchor that was adopted in the full-scale sherwall tests. The CLT specimens were loaded parallel to the direction of their outer layers. A symmetric layout of the test was ensured by connecting two hold-downs to each side of the specimen, as shown in Figure 7. The hold-downs were connected to the 400x700x100 mm CLT specimen using fifty-five 4x60 ring shanked nails. Four LVDTs (two one each side) were used to measure the vertical displacement of the CLT specimens relative to the base of the hold-down anchor.

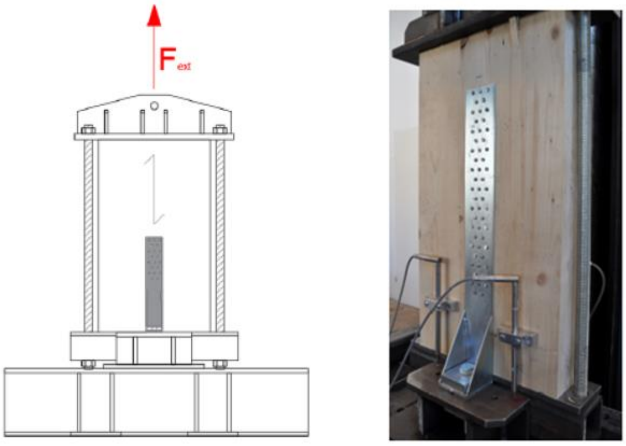


**Figure 7:** *tests on hold-down*

# 4. Experimental results and discussion

## <u>4.1 Shearwall tests</u>

All shearwall specimens were loaded until failure was documented in either the hold-down or lintel beam. The loading protocol persisted beyond potential initial cracks in the lintel beams until the ultimate failure was reached in order to detect any possible change in failure mode during the testing process. Failure in the hold-downs was characterised by a relatively brittle tensile failure in the steel plate along the bottom row of the nails, as shown in Figure 8.

**Figure 8:** *hold-down failure in Wall 03 (W_5_S)*

The failure in the lintel beam was characterised by a net shear or bending failure. The net shear failure was observed to occur at the end of the lintel section (i.e. near the wall segment) in all horizontal layers, as shown in Figure 9 for Wall 01 (D_3_S). The bending failure was observed to correspond to finger joints in the inner horizontal boards at the end of the lintel section, as shown in Figure 10 for Wall 04 (D_3_L).


**Figure 9:** *failure in the lintel of Wall 01 (D_3_S)*

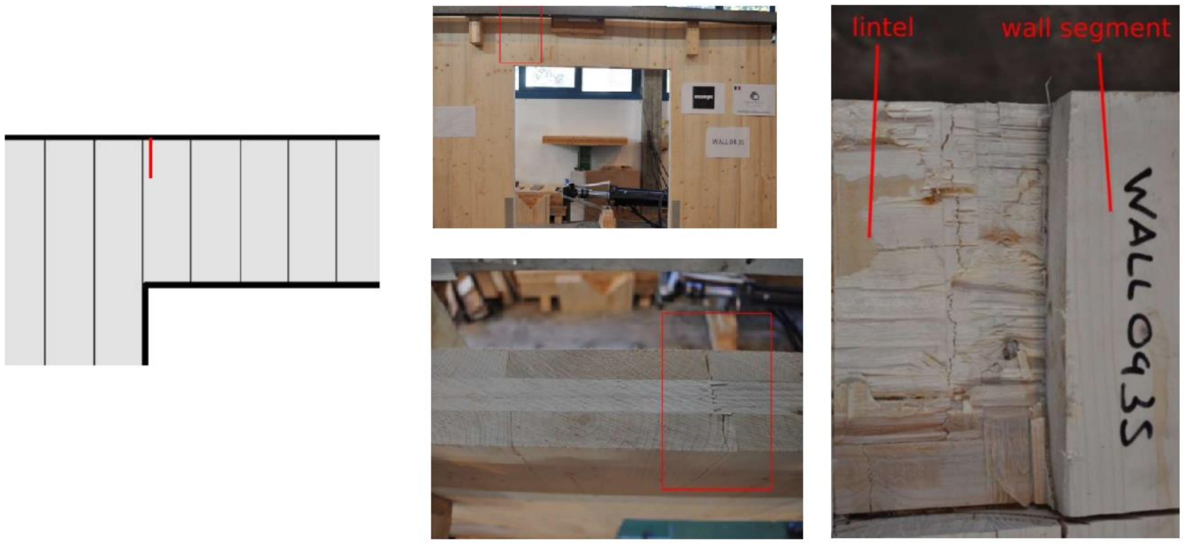


**Figure 10:** *failure in the lintel of Wall 04 (D_3_L)*

The load-displacement curves for all the tested walls are shown in Figure 11, where the point at which the hold-down anchor (HD) or the CLT lintel beam fails are indicated. In general, it can be observed that the behaviour is brittle since it is influenced by failure in the hold-down or the lintel beam, both of which have brittle behaviour. Although the failure in the CLT panel is expected to be brittle, the behaviour of the hold-down depends on their nailing configuration. In the current study, and in order to observe failure in the lintel beam, commercially available fully-nailed hold downs were adopted, which led to the brittle failure observed. Other hold-downs may possess more ductility (e.g. partially nailed) and therefore prioritizing failure in the hold-down rather than the CLT panel is preferred in design because the overall behaviour of the wall assembly could be better controlled. Failure in the CLT panel will always be brittle and therefore it should be avoided when possible.

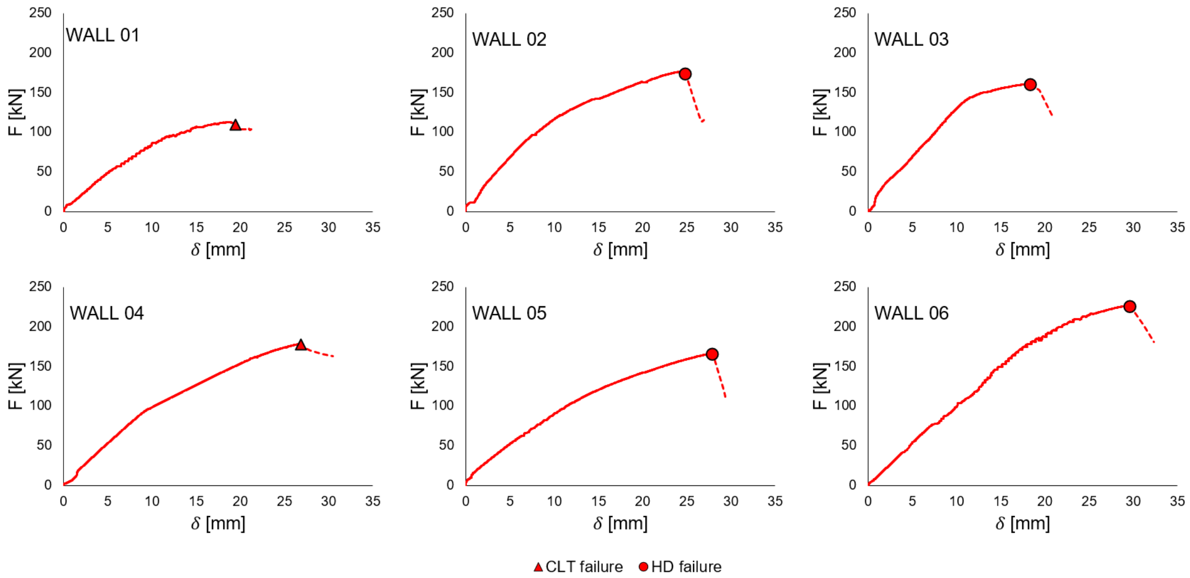


**Figure 11:** *force vs displacement curves of full scale shearwall specimens.*

Experimental results, including maximum load, $F_{max}$, and corresponding displacement, $\delta_{F_{max}}$, load and displacement corresponding to the hold-down failure, $F_{u,hd}$ and $\delta_{u,hd}$, load and the displacement corresponding to failure in the CLT panel, $F_{u,CLT}$ and $\delta_{u,CLT}$, and the lateral stiffness of the shearwall, k, calculated as the slope between 10% and 40% of the maximum load, are reported in Table 3.

**Table 3:** *mechanical parameter obtained from the force-displacement curve*

| Test | Label | Failure mode | $F_{max}$ [kN] | $\delta_{F_{max}}$ [mm] | $F_{u,CLT}$ [kN] | $\delta_{u,CLT}$ [mm] | $F_{u,hd}$ [kN] | $\delta_{u,hd}$ [mm] | k [kN/mm] |
|---|---|---|---|---|---|---|---|---|---|
| Wall 01 | D_3_S | CLT panel | 113 | 18.4 | 106 | 19.7 | - | - | 9.54 |
| Wall 02 | D_5_S | Hold-down | 176 | 24.3 | - | - | 174 | 24.8 | 13.71 |
| Wall 03 | W_5_S | Hold-down | 161 | 18.1 | - | - | 160 | 18.3 | 12.58 |
| Wall 04 | D_3_L | CLT panel | 179 | 26.8 | 179 | 26.8 | - | - | 10.25 |
| Wall 05 | D_5_L | Hold-down | 166 | 27.7 | - | - | 166 | 27.7 | 8.64 |
| Wall 06 | W_5_L | Hold-down | 227 | 29.4 | - | - | 227 | 29.4 | 9.66 |

With the exception of Wall 03 (specimen W_5_S), the deformed shapes for all the other tested shearwalls were characterized by two centres of rotation, one at each wall segment, as shown in Figure 12a for Wall 01 (D_3_S). This observation was possible due to the monitoring of the uplift displacement, $v_1$, which had a relatively small negative value, implying compression forces at that location. The bottom edge of the shearwall at the opposite end was, as expected, always in compression. Wall 03 exhibited a kinematic mode consistent with the other shearwalls initially, however after 10 mm of horizontal displacement, the wall behaviour shifted to that of single centre of rotation, , as shown in Figure 12b, which coincided with the yielding of the nails in the hold-down.

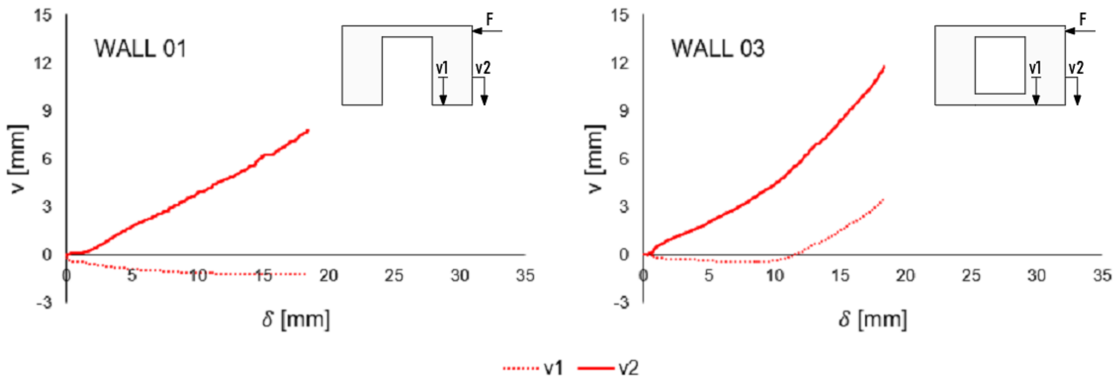


**Figure 12:** *uplifts in outermost wall segments for Wall 01 (a) and Wall 03 (b)*

## 4.2 Component-level tests

As anticipated, all beam specimens with length equal to $l_{beam}$ = 4760 mm (i.e. B 01 and B 02), failed in bending, and the failure occurred near the mid-span of the beam elements, as shown in Figure 13. The failure mode in the beam specimens with length equal to $l_{beam}$ = 2720 mm (i.e. B03 and B04) was less consistent and involved bending failure in one of the specimens (#1 for B03 and #1 for B04), while net shear failures in the two horizontal laminations was observed in the other two specimens (#2 and #3 for B03, #2 and #3 for B04), as shown in Figures 14 and 15.


**Figure 13:** *failure mode in long beams, B 02 (specimen #2),a, and B 01 (specimen #3),b.*

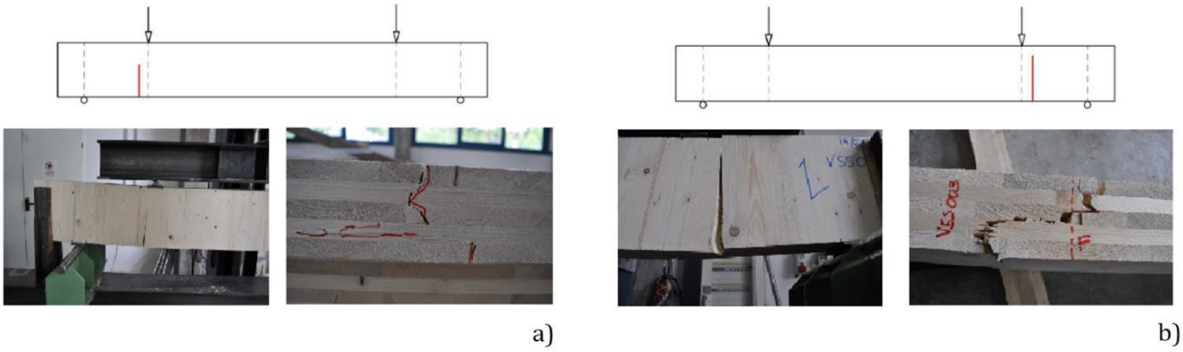


**Figure 14:** *tests on short beams B 03 (specimen #2),a, and B 03 (specimen #3),b.*

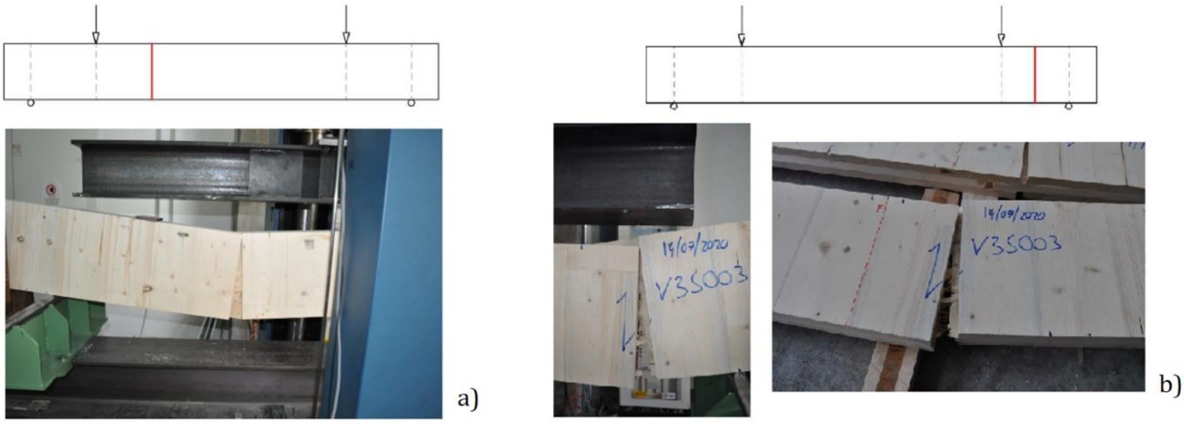


**Figure 15:** *tests on short beams B 04 (specimen #1),a, and B 04 (specimen #3),b.*

Table 4 presents the results obtained from the beam tests, including maximum load, $F_{max}$, and the corresponding failure.

**Table 4:** *maximum load and failure mode of CLT beam tests*

| *Configuration and Test* | | | $F_{max}$ [kN] | *Failure mode* |
|---|---|---|---|---|
| $l_{beam}$ = 4760 mm | B 01 | #1 | 61.1 | Bending |
| | | #2 | 52.3 | Bending |
| | | #3 | 57.3 | Bending |
| | B 02 | #1 | 60.0 | Bending |
| | | #2 | 19.5 | Bending |
| | | #3 | 44.3 | Bending |
| $l_{beam}$ = 2720 mm | B 03 | #1 | 172.9 | Bending |
| | | #2 | 180.8 | Net shear |
| | | #3 | 217.4 | Net shear |
| | B 04 | #1 | 111.7 | Bending |
| | | #2 | 118.2 | Net shear |
| | | #3 | 128.8 | Net shear |

Table 5 provides the effective local modulus of elasticity along the major direction, $E_l$, calculated based on a linear regression between the 10% and 40% of the maximum load, according to EN408 [26], and considering only the contribution of horizontal layers when calculating the area moment of inertia $I_{net}$, as presented in Equation (1):

$$I_{net} = \frac{t_h \cdot h^3}{12} \tag{1}$$

The bending strength of the beams, $f_m$, obtained from the maximum load on beams with lengths $l_{beam}$ = 4760 mm, was calculated using Equation 2.

$$f_m = \frac{M_{max}}{W_{net,h}} \tag{2}$$

where the maximum bending moment, $M_{max}$, and the elastic section modulus, $W_{net}$, are calculated, as shown in Equation (3) and (4), respectively:

$$M_{max} = \frac{F_{max} \cdot a}{2} \tag{3}$$

$$W_{net} = \frac{t_h \cdot h^2}{6} \tag{4}$$

where $a$ is the distance between the support and the load application point, equalling 1360 mm.

It can be noted that the variability for beam B 02 is very high, even though the mean value obtained is consistent with the expected average bending strength. Since only six tests have been conducted and the current study is one of the first of its kind to address the behaviour of CLT beams with vertical outer laminations, it cannot be determined with certainty whether some of the values obtained represent outliers. All data points are presented here to allow future studies by the authors and others to evaluate this observation further.

**Table 5:** *local modulus of elasticity and bending strength*

| *Test* | | | $E_l$ | *Mean* | *CoV* | $f_m$ | *Mean* | *CoV* |
|---|---|---|---|---|---|---|---|---|
| | | | *[MPa]* | *[MPa]* | *[-]* | *[MPa]* | *[MPa]* | *[-]* |
| $l_{beam}$ = 4760 mm | *B 01* | *#1* | *14071* | | | *53.9* | | |
| | | *#2* | *14006* | *13878* | *2%* | *46.1* | *50.2* | *8%* |
| | | *#3* | *13558* | | | *50.5* | | |
| | *B 02* | *#1* | *14286* | | | *70.6* | | |
| | | *#2* | *12062* | *13411* | *9%* | *22.9* | *48.5* | *50%* |
| | | *#3* | *13886* | | | *52.1* | | |

From the tests on beams with lengths $l_{beam}$ = 2720 mm, the net shear strength capacity $f_v$ was calculated and presented in Table 6 by assuming a parabolic distribution of the internal shear stress according to the Jourawski theory [31], as presented in Equation (5).

$$f_v = \frac{3}{2} \cdot \frac{\frac{F_{max}}{2}}{t_{net} \cdot h} \tag{5}$$

where $t_{net} = \min(t_h; t_v)$.

The torsional shear strength capacity $f_T$ was not determined since no failure due to torsional shear between lamination was observed in the tests. When a shear failure mode did not occur in the shear tests, $f_v$ represents the lower bound value of the net shear strength capacity.

**Table 6:** *net shear strength*

| *Test* | | | *Failure mode* | $f_v$ |
|---|---|---|---|---|
| | | | | |
| $l_{beam}$ = 2720 mm | *B 03* | *#1* | *Bending* | *>9.3* |
| | | *#2* | *Net shear* | *10.0* |
| | | *#3* | *Net shear* | *12.0* |
| | *B 04* | *#1* | *Bending* | *>8.2* |
| | | *#2* | *Net shear* | *8.7* |
| | | *#3* | *Net shear* | *9.5* |

A relatively brittle failure was observed in the net section of the hold down steel plate. The maximum load, $F_{max}$, and the corresponding displacement, $v_{Fmax}$, as well as the lateral stiffness, $k_{el}$, are reported in Table 7 and the average load-displacement curve obtained from the tests is shown in Figure 16.

**Table 7:** *hold-down elastic stiffness and ultimate load and displacement*

| ID test | $k_{el}$ | $F_{max}$ | $v_{Fmax}$ |
|---|---|---|---|
| [-] | [kN/mm] | [kN] | [mm] |
| #1 | 15.3 | 98.7 | 11.9 |
| #2 | 9.8 | 93.9 | 14.4 |
| **Mean** | **12.3** | **94.9** | **12.00** |

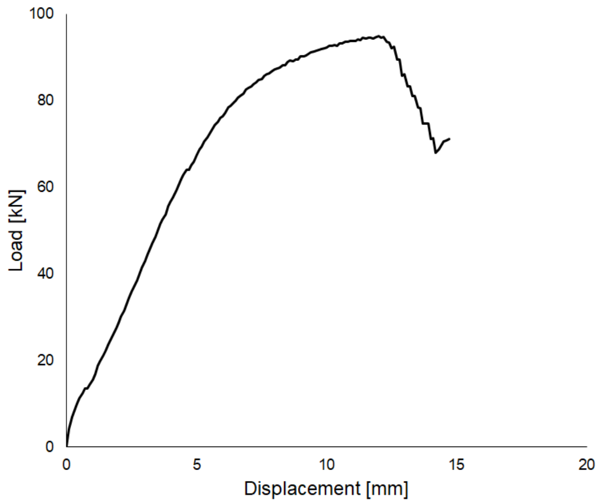


**Figure 16:** *load-displacement average curve from tensile tests on hold-down*

## 5. Numerical analysis

### 5.1 Description of the model

Numerical models were developed in the software package SAP2000 [27] to simulate the mechanical behaviour and failure modes of the tested CLT shearwalls. The methodology used in the model is consistent with that reported in [14,20]**.** Four-joints quadrilateral homogeneous shell elements with a mesh size equal to 37.5 x 37.5 mm were adopted for the modelling of the in-plane behaviour of the CLT panels. An example of the numerical model for Wall 02 (D_5_S) can be seen in Figure 17. The thickness of the shell elements was taken equal to the thickness of the wall CLT panel. Linear elastic orthotropic material properties were assigned to the shell elements. Effective modulus of elasticity $\boldsymbol{E_{eff,h}}$ and $\boldsymbol{E_{eff,v}}$ for the two in-plane directions were defined to take into account the different CLT panel layups as expressed by Equations 6 and 7:

$$E_{eff,h} = \frac{E_0 \cdot t_h}{t_{tot}} \text{ along the horizontal direction} \tag{6}$$

$$E_{eff,v} = \frac{E_0 \cdot t_v}{t_{tot}} \text{ along the vertical direction} \tag{7}$$

where $\boldsymbol{E_0}$ is the mean value of modulus of elasticity parallel to the grain obtained from the beam tests. $\boldsymbol{t_{tot}}$ is the total thickness of the panel, while $\boldsymbol{t_h}$ and $\boldsymbol{t_v}$ represent is the total thickness of the horizontal and vertical layers, respectively. An effective in-plane shear modulus, $\boldsymbol{G_{eff}}$, was determined according to the Equation 8, which takes into account both shear and torsional deformations of the laminations, as proposed by Brandner et al. [28].

$$G_{eff} = \frac{G_0}{1+6 \cdot \alpha_T \cdot \left(\frac{t_{mean}}{w}\right)^2} \tag{8}$$

where $G_0$ is the shear modulus of the laminations, obtained from EN 338 [29], $w$ is the width of laminations, $t_{mean}$ is the mean thickness of laminations, calculated according to Equation 9, and $\alpha_T$ is obtain using Equation 10.

$$t_{mean} = \frac{t_{tot}}{N} \tag{9}$$

$$\alpha_T = p \cdot \left(\frac{t_{mean}}{w}\right)^q \tag{10}$$

where $N$ is the number of layers, $q$ is equal to -0.79 and $p$ is equal to 0.53 and 0.43 for 3 and 5 layers of the CLT panel, respectively, as reported in [28]. The values of $E_{eff,h}$, $E_{eff,v}$ and $G_{eff}$ are reported in Table 8 for each panel layups.

**Table 8:** *values of equivalent modulus for each layup of CLT panels*

| $t_{tot}$ | N | layup | $E_0$ | $G_0$ | $t_h$ | $t_v$ | $E_{eff,h}$ | $E_{eff,v}$ | $G_{eff}$ |
|---|---|---|---|---|---|---|---|---|---|
| [mm] | [-] | [-] | [MPa] | [MPa] | [mm] | [mm] | [MPa] | [MPa] | [MPa] |
| 100 | 5 | 20v-20h-20v-20h-20v | 13878 | 690 | 40 | 60 | 5551 | 8327 | 578 |
| 90 | 3 | 30v-30h-30v | 13411 | 690 | 30 | 60 | 4470 | 8940 | 494 |

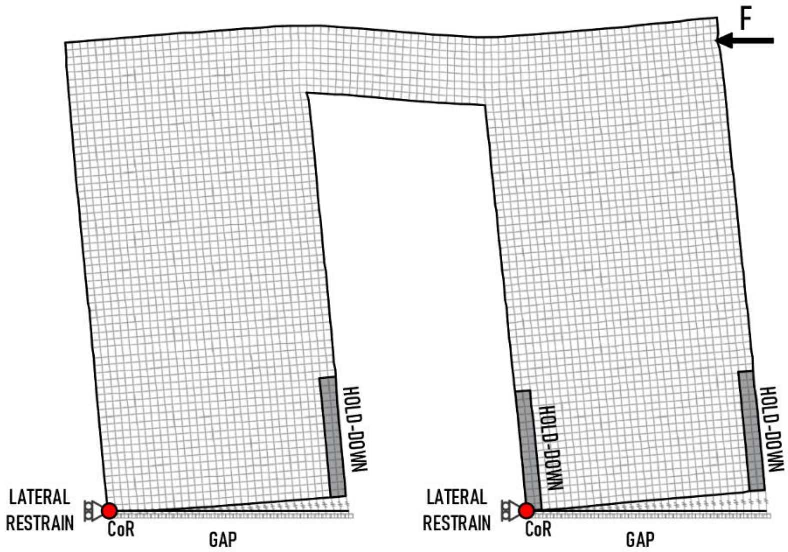


**Figure 17:** *FE numerical model for Wall 02 (D_5_S)*

Each hold-down was modelled using 1-joint multi-linear elastic link element with mechanical behaviour represented by the average load-displacement curve obtained from the two tensile tests reported in Section 4. Rigid compression-only (i.e. gap) elements, located along the base of the shearwall, were used to simulate the contact between the CLT panels and the steel base beam. Rigid horizontal restraints were applied at bottom corners of the wall segments in a manner consistent with those found in the wall tests, as shown in Figure 3. A displacement-controlled non-linear static analysis was performed by increasing the lateral displacement at the top of the shearwall.

## 5.2 Prediction Investigation of failure modes

The failure condition related to the CLT panels was determined by means of a step-by-step verification of the axial ($n_h$ and $n_v$) and shear ($v$) internal forces per unit length in the shell elements, according to Equation 11.

$$n_h = n_{R,h};\ \ n_v = n_{R,v};\ v = v_R \quad (11)$$

where $n_{R,h}$, $n_{R,v}$ are the axial strength per unit length in the horizontal and vertical directions, respectively, and $v_R$ is the shear strength per unit length. The axial strength per unit length can be calculated according to Equations 12 and 13 as the product of either the tensile, $f_{t,CLT}$, or compressive, $f_{c,CLT}$, strength of laminations and the total thickness along the horizontal, $t_h$, and vertical, $t_v$, direction, respectively.

$$n_{R,h} = \begin{cases} f_{t,CLT} \cdot t_h\ ,\ if\ n_h \geq 0 \\ f_{c,CLT} \cdot t_h\ ,\ if\ n_h < 0 \end{cases} \quad (12)$$

$$n_{R,v} = \begin{cases} f_{t,CLT} \cdot t_v\ ,\ if\ n_v \geq 0 \\ f_{c,CLT} \cdot t_v\ ,\ if\ n_v < 0 \end{cases} \quad (13)$$

The net shear strength, $v_{R,net}$, and the torsional shear strength, $v_{R,tor}$, can be obtained as expressed by Equations 14 and 15:

$$v_{R,net} = f_v \cdot min(t_h, t_v) \quad (14)$$

$$v_{R,tor} = min\left(\frac{f_{tor} \cdot w \cdot t_v \cdot n_{CA,i}}{3 \cdot t_{v,i}}\right) \quad \textit{for i=1, 3 and 5} \quad (15)$$

where $f_v$ is the mean value of the net shear strength obtained from the beam tests, $n_{CA,i}$ is the number of crossing area that the i-th vertical layer shares with adjacent layers, $f_{tor}$ is the mean value of the torsional strength and $t_{v,i}$ is the thickness of the *i-th* vertical layer.

It is noteworthy to mention that the variables $n_{R,h}$ and $n_{R,v}$ represent the strength capacities of the CLT panel subjected to a pure compressive or tensile force, which acts uniformly along the entire section. In the case being investigated, the CLT elements are subjected primarily to bending, and as such, the bending strength capacity is more appropriate in the determination of strength capacity of the element [34]. Also, since the outputs from shell elements are expressed in terms of axial internal forces per unit length, $f_{c,CLT}$ and $f_{t,CLT}$, in Equations 12 and 13 have been replaced with the bending strength, $f_{m,CLT}$, obtained from the beam tests presented in Section 2. The axial strength per unit length can hence be calculated as expressed by Equations 16 and 17.

$$n_{R,h} = f_{m,CLT} \cdot t_h \qquad (16)$$

$$n_{R,v} = f_{m,CLT} \cdot t_v \qquad (17)$$

It was observed from the experimental tests on CLT beams that the shear failure mechanism was related to a net shear failure. This is likely due to the values of width-to-thickness ratio adopted in the experimental campaign, which ensured that torsional shear failure mechanism was supressed. The axial and shear strength per unit length, calculated according to the equations presented in this section, are reported in Table 9 for each panel layup.

**Table 9:** *axial and shear strength per unit length of the CLT panels*

| $t_{tot}$ | $N$ | layup | $f_{m,CLT}$ | $f_{v,CLT}$ | $t_h$ | $t_v$ | $n_{R,h}$ | $n_{R,v}$ | $v_R$ |
|---|---|---|---|---|---|---|---|---|---|
| [mm] | [-] | [-] | [MPa] | [MPa] | [mm] | [mm] | [kN/m] | [kN/m] | [kN/m] |
| 100 | 5 | 20v-20h-20v-20h-20v | 50.20 | 10.96 | 40 | 60 | 2008 | 3012 | 438 |
| 90 | 3 | 30v-30h-30v | 48.52 | 9.08 | 30 | 60 | 1456 | 2911 | 272 |

As mentioned before, the magnitude of stress obtained from the numerical model near the corner zones is not representative of the local real stresses. The values given by numerical model are notoriously much higher than the values expected to be experienced by the physical test specimen. This phenomenon has also been highlighted and discussed by other studies dealing with interpretation of numerical data [30]. For this reason, the verifications were performed by excluding a distance from the edge of the CLT panel, equal to the mesh size (37.5 mm), which corresponds approximately to 10% of the height of the section. Although, as will be presented in the next section, this approach seems to provide accurate and realistic predictions of the internal stresses, further studies are needed to investigate the internal stress distribution.

### 5.3 Validation of the FE models

The validation of the proposed procedure in the numerical models was carried out by comparing the results obtained from the analyses with those from shearwall tests in terms of failure modes, load-displacement curves, number of centre of rotations as well as deformation in the CLT panels.

The comparisons between the load-displacement curves obtained from the test results and FE models are presented in Figure 18. Additionally, numerical comparisons in terms of wall stiffness, $K$, maximum shear force, $F_{max}$, mode of failure and number of centres of rotation (CoR) at ultimate displacement are reported in Table 10. The percentage difference $\varepsilon$ is calculated and reported for the stiffness and strength values. Also provided in Table 10 is the reserved capacity (i.e. overcapacity - OC) of the component (hold-down or CLT panel) that did not govern the failure of the wall, obtained from the FE models.

**Table 10:** *comparison between FE analyses and experimental tests*

| | | $K$ [kN/mm] | | | $F_{max}$ [kN] | | | failure mode | | *CoR* | | *OC of unfailed component* | |
|---|---|---|---|---|---|---|---|---|---|---|---|---|---|
| Test | Label | FE | test | $\varepsilon$ [%] | FE | test | $\varepsilon$ [%] | FE | test | FE | test | Component | OC [-] |
| Wall 01 | D_3_S | 7.8 | 9.5 | -17.7 | 97.8 | 112.8 | -13.3 | CLT shear | CLT shear | 2 | 2 | HD | 1.20 |
| Wall 02 | D_5_S | 9.1 | 13.7 | -33.7 | 182.2 | 176.5 | 3.2 | HD | HD | 2 | 2 | CLT | 1.02 |
| Wall 03 | W_5_S | 9.5 | 12.8 | -25.9 | 136.0 | 160.9 | -15.5 | HD | HD | 1 | 1 | CLT | 1.79 |
| Wall 04 | D_L_L | 9.1 | 10.2 | -11.1 | 171.1 | 178.6 | -4.2 | CLT shear | CLT bending | 2 | 2 | HD | 1.03 |
| Wall 05 | D_5_L | 8.6 | 8.6 | 0.1 | 162.0 | 165.9 | -2.4 | HD | HD | 2 | 2 | CLT | 1.18 |
| Wall 06 | W_5_L | 9.8 | 9.7 | 1.8 | 240.0 | 226.8 | 5.8 | HD | HD | 2 | 2 | CLT | 1.01 |

From Table 10, it can be observed that the maximum discrepancy between the model and test results regarding the maximum load is 15.5%. This is considered reasonable provided the variability found in wood and hold-down connectors. The comparison of the initial stiffness shows more variability, which is expected since stiffness is notoriously more difficult to estimate. The model prediction of the failure mode is accurate for all the studied specimens, which is an important and encouraging finding as it presents another evidence of the appropriateness of the proposed modelling procedure. Similarly, the model was capable of correctly predicting the number of centre of rotations at the ultimate condition. It is noteworthy to mention that for shearwalls 01, 03 and 05 the overcapacity of the unfailed component is quite large, indicating that a clear failure mode was obtained from the models. Conversely, for shearwalls 02, 04 and 06, the values of overcapacity of the unfailed component is close to unity, showing a more balanced failure mode between CLT panel and hold-down.

The comparison presented in Figure 18 shows that the prediction of the model is quite reasonable. In general, predicting the overall behaviour and failure point in wall specimens, where the failure occurred in the CLT lintel beam (Walls 01 and 04), seems less accurate than when the failure occurred in the hold-down anchors (Walls 02, 03, 05 and 06). This is expected since less variability is associated with failure in the steel bracket in the hold-down.

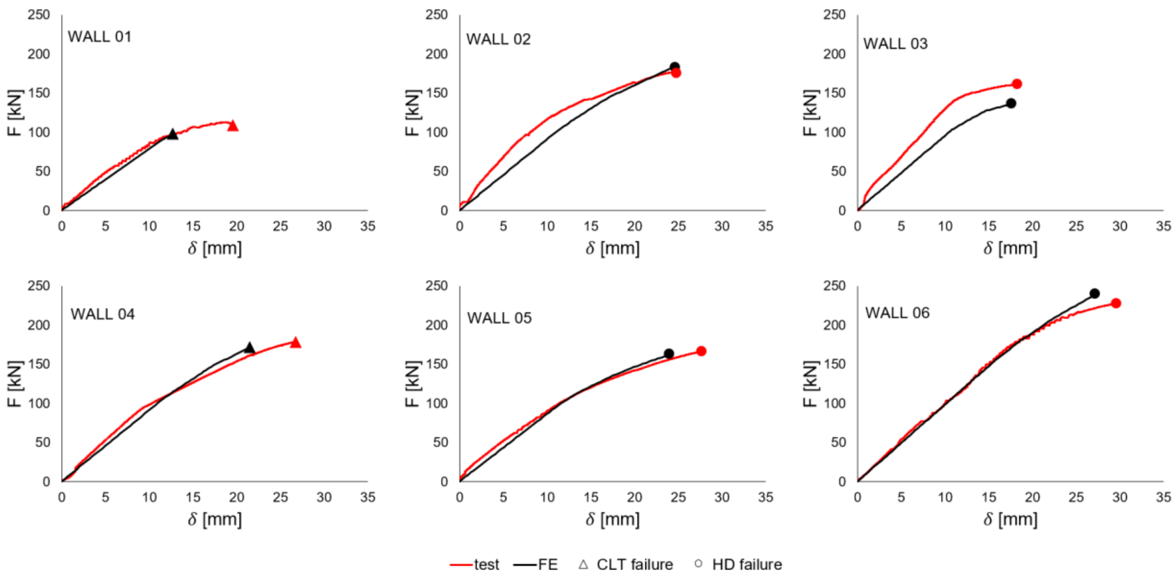


**Figure 18:** *comparison between the load-displacement curves of FE model and experimental test*

It should be noted that the distribution of the internal horizontal axial and shear forces were obtained at the points where the values of internal forces exceeded the strength values, $n_{R,h}$ and $v_R$ (Equations 14, 15 and 17), as shown in Figures 19 for Wall 01 and 04, respectively. The values are selected at the analysis step corresponding to the failure point represented in Figure 18.

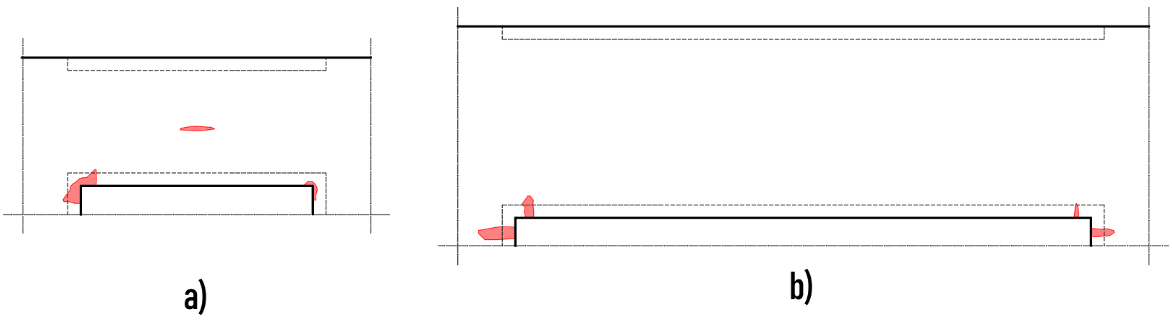


**Figure 19:** *distribution of shear forces greater than the corresponding strength capacities detected at the ultimate condition for Wall 01 (a) and Wall 04 (b).*

The displacements measured by the two diagonal LVTDs attached to the CLT panel in the experimental tests were compared to those obtained from the FE model, as shown in Figure 20. The values from the FE model were obtained by determining the relative displacement between the joints where the diagonal LVTDs were attached on the shearwall. It can be seen that a good accuracy was obtained, showing the reliability of the methodology used to model the CLT panels by means of homogenous shell elements with effective moduli of elasticity and effective shear modulus. It is particularly noteworthy to mention that the proposed methodology is adequate even when significant deformations are observed in the CLT panels due to openings. In general, since relatively small deformations are observed in shearwalls without openings, even significant deviations in estimating the panel deformation have little effect on the overall prediction. Contrarily, the flexibility of the lintel beam in shearwall with openings leads to an overall panel flexibility that cannot be ignored in the analysis. As such, the obtained results in the study related to the deformation along the diagonals of the shearwall, can also be considered novel and further emphasizes the adequacy of the proposed model.

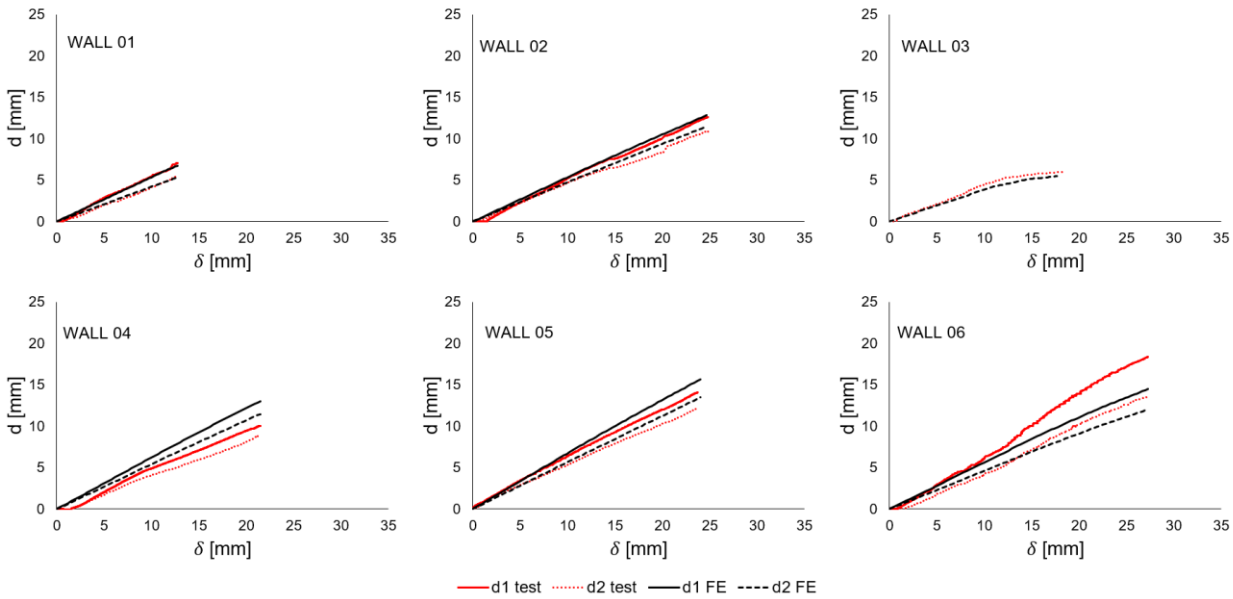


**Figure 20:** *test and FE mesurement of diagonals*

## 6. Conclusions

In this study, the mechanical behaviour of CLT shearwalls, where either door or window openings are cut out of the panels, is investigated through full-scale experimental tests and numerical analyses. The main conclusions that can be drawn from the current study are:

- experimental tests showed that failure mode of CLT shearwalls with openings can occur either in mechanical anchors or in the CLT panels, depending on the geometrical dimensions and mechanical properties of the shearwalls. Differently from single-panel shearwalls with no openings, the brittle failure in the CLT panels is a possible mode of failure that designers need to consider;
- the failure mode in the CLT panels was observed to occur either in bending or net shear in the lintel beam, depending on the layup pattern, number of layers, orientation of laminates and the geometrical and mechanical properties of the shearwall. Although based on the current investigation failure mode in wall segments and parapets seems less likely, potential future work should consider such failure modes;
- the proposed numerical procedure was capable of predicting the maximum load with reasonable accuracy, provided the variability found in wood and hold-down connectors. The model prediction of the failure mode, number of centre of rotations, and the overall deformation of the CLT panel was accurate for all the studied specimens.

## Acknowledgments

Silvio Pedrotti and Giorgio Gislimberti from ESSEPI srl (Italy) are acknowledged for providing all the CLT specimens in the experimental tests on both beam and shearwalls. CSI Italia srl is acknowledged for providing the software SAP2000 used in this work for the implementation of the numerical models. A special thank goes to Raniero Leendert Casesa (University of Trieste, Italy) for their help in the pre- and post-processing of experimental data on shearwall tests and the numerical analyses. Diego Magnago and Mario Pinna are acknowledged for running all the tests.

## References


[1] Brandner R, Flatscher G, Ringhofer A, Schickhofer G, Thiel A. (2016) Cross laminated timber (CLT): overview and development. Eur J Wood Wood Prod,2016;74(3):331–51. http://dx.doi.org/10.1007/s00107-015-0999-5.

[2] Izzi M, Casagrande D, Bezzi S et al. (2018) Seismic behaviour of cross-laminated timber structures: a state-of-the-art review. Engineering Structures 170: 42–52.

[3] Ceccotti A, Sandhaas C, Okabe M, Yasumura M, Minowa C, Kawai N (2013) SOFIE project– 3D shaking table test on a seven-storey full-scale cross-laminated building.Earthquake Eng Struct Dyn 2013;42(13):2003–21. http://dx.doi.org/10.1002/eqe.2309.

[4] Tsuchimoto T, Kawai N, Yasumura M, Miyake T, Isoda H, Tsuda C, Miura S, Murakami S, Nakagawa T. (2014) Dynamic and static lateral load tests on full-sized 3-story CLT construction for seismic design. In: World Conference on Timber Engineering (WCTE), Quebec City, Quebec, Canada; 2014.

[5] Flatscher G, Schickhofer G (2015) Shaking-table test of a cross-laminated timber structure. Proc ICE Struct Build 2015;168(11):878–88. http://dx.doi.org/10.1680/stbu.13.00086.

[6] Popovski M, Gavric I (2016) Performance of a 2-story CLT house subjected to lateral loads.J Struct Eng 2016;142(4):E4015006. http://dx.doi.org/10.1061/(ASCE)ST.1943-541X.0001315.

[7] van de Lindt JW, Furley J, Amini MO, Pei S, Tamagnone G, Barbosa AR, Rammer D, (...), Popovski M (2019) Experimental seismic behavior of a two-story CLT platform building (2019) Engineering Structures, 183, pp. 408-422. doi: 10.1016/j.engstruct.2018.12.079

[8] Popovski M, Schneider J, Schweinsteiger M. (2010) Lateral load resistance of cross-laminatedwood panels. In: World Conference on Timber Engineering (WCTE), Riva delGarda, Italy; 2010.

[9] Hristovski V, Dujic B, Stojmanovska M, Mircevska V (2013) Full-scale shaking-table testsof XLam panel systems and numerical verification: Specimen 1. J Struct Eng 2013;139(11):2010–8. http://dx.doi.org/10.1061/(ASCE)ST.1943-541X.0000754.

[10] Okabe M, Yasumura M, Kobayashi K, Haramiishi T, Nakashima Y, Fujita K. Effect ofvertical load under cyclic lateral load test for evaluating Sugi CLT wall panel. In:World Conference on Timber Engineering (WCTE), Auckland, New Zealand; 2012.

[11] Gavric I, Fragiacomo M and Ceccotti A (2015) Cyclic behavior of CLTwall systems: experimental tests and analytical prediction models. Journal of Structural Engineering 141(11): 04015034. https://doi.org/10.1061/(ASCE)ST.1943-541X.0001246.

[12] Akbas T, Sause R, Ricles JM, Ganey R, Berman J, Loftus S, Dolan JD, (...), Blomgren, H E (2017) Analytical and Experimental Lateral-Load Response of Self-Centering Posttensioned CLT Walls (2017) Journal of Structural Engineering (United States), 143 (6), art. no. 04017019. doi: 10.1061/(ASCE)ST.1943-541X.0001733

[13] Chen Z, Popovski M (2020) Mechanics-based analytical models for balloon-type cross-laminated timber (CLT) shear walls under lateral loads (2020) Engineering Structures, 208, art. no. 109916. doi: 10.1016/j.engstruct.2019.109916

[14] D'Arenzo G, Casagrande D, Polastri A, Fossetti M, Fragiacomo M, Seim W (2021) CLT shearwalls anchored with shear-tension angle brackets: experimental tests and finite element modelling, Journal of Structural Engineering, ASCE, 147(7), 04021089 doi: 10.1061/(ASCE)ST.1943-541X.0003008.

[15] Dujic B, Klobcar S and Zarnic R (2007) Influence of openings on shear capacity of wooden walls. Proceedings of 40th CIB-W18 Meeting, Bled, Slovenia, paper 40-15-6.

[16] Ceccotti A, Lauriola M, Pinna M and Sandhaas C (2006) SOFIE project – cyclic tests on cross-laminated wooden panels. Proceedings of World Conference on Timber Engineering (WCTE), Portland, OR, USA, vol. 1, pp. 805–812.

[17] Flatscher G, Bratulic K and Schickhofer G (2015) Experimental tests on cross-laminated timber joints and walls. Proceedings of the Institution of Civil Engineers – Structures and Buildings 168(11): 868–877, https://doi.org/10.1680/stbu.13.00085.

[18] Yasumura M, Kobayashi K, Okabe M, Miyake T, Matsumoto K (2016) Full-scale tests and numerical analysis of low-rise CLT structures under lateral loading. J Struct Eng 2016;142(4):E4015007. http://dx.doi.org/10.1061/(ASCE)ST.1943-541X. 0001348.

[19] Pai S, Lam F, Haukaas T (2017) Force transfer around openings in cross-laminated timber shear walls. J Struct Eng 2017;143(4):04016215. https://doi.org/10.1061/(ASCE)ST.1943-541X.0001674.

[20] Mestar M, Doudak G, Polastri A, Casagrande D (2021) Investigating the kinematic modes of CLT shearwalls with openings, Engineering Structures, 2021, 228, 111475, doi: 10.1016/j.engstruct.2020.111475

[21] Moosbrugger T et al. 82006) Cross-laminated timber wall segments under homogeneous shear - with and without openings. WCTE 2006, 9th world conference on timberengineering. Portland, Oregon, United States; 2006.

[22] Dujic B, Klobcar S and Zarnic R (2007) Influence of openings on shear capacity of wooden walls. Proceedings of 40th CIB-W18 Meeting, Bled, Slovenia, paper 40-15-6.

[23] Shahnewaz M, Alam MS, Tannert T and Popovski M (2016) Cross laminated timber walls with openings: inn-plane stiffness prediction and sensitivity analysis. Proceedings of 5th International Structural Specialty Conference, CSCE, At London, ON, USA, vol. 4, pp. 2943–2952.

[24] Mestar M, Doudak G, Caola M, Casagrande D (2020) Equivalent-frame model for elastic behaviour of cross-laminated timber walls with openings (2020) Proceedings of the Institution of Civil Engineers: Structures and Buildings, 173 (5), pp. 363-378. doi: 10.1680/jstbu.19.00057

[25] CEN (2011) Timber Structures – Test Methods – Racking Strength and Stiffness of Timber Frame Wall Panels, EN 594. . European Committee for Standardization: Brussels, Belgium

[26] CEN (2012) Timber structures-Structural Timber and Glued Laminated Timber-Determination of Some Physical and Mechanical Properties. EN 408. European Committee for Standardization: Brussels, Belgium

[27] CSI (2017) SAP2000 Integrated Software for Structural Analysis and Design. Berkeley,California: Computers and Structures Inc.; 2017.

[28] Brandner R, Dietsch P, Dröscher J et al. (2017) Cross laminated timber (CLT) diaphragms under shear: test configuration, properties and design. Construction and Building Materials 147: 312–327.

[29] CEN (2016) Structural timber- Strength classes, EN 338. European Committee for Standardization: Brussels, Belgium

[30] Casagrande D, Fanti R, Greco M, Gavric I, Polastri A (2021) On the distribution of internal forces in single-storey CLT symmetric shearwalls with openings, submitted to Structures Journal, Elsevier, **Unpublished results.**

[31] Jourawski D J (1856). Sur la résistance d'un corps prismatique et d'une pièce composée en bois ou en tôle de fer à une force perpendiculaire à leur longueur.Mèmoires Annales des Ponts et Chaussées 2, 328-351

[32] Gavric I , Popovski M (2014), Design models for CLT shearwalls and assemblies based on connection properties. Proc. Meet. 47, INTER- Int. Netw. Timber Eng. Res., no. January, pp. 269-280, 2014.

[33] ETA 12/0362 (2020) European Technical Approval: Cross Laminated Timber (CLT) – Solid wood slab elements to be used as structural elements in buildings, Essepi XXL. Eurofins Expert Services Oy, Finland.

[34] ETA 12/0347 (2017) European Technical Approval: Cross Laminated Timber (CLT) – Solid wood slab elements to be used as structural elements in buildings, XLAM Dolomiti CLT. Osterreichisches Institut fur Bautechcnik, Vienna, Austria.